Original Article

Effects of Diabetes on Ryanodine Receptor Ca Release Channel (RyR2) and Ca^{2+} Homeostasis in Rat Heart

Nazmi Yaras,[1] Mehmet Ugur,[1] Semir Ozdemir,[1] Hakan Gurdal,[2] Nuhan Purali,[3] Alain Lacampagne,[4] Guy Vassort,[4] and Belma Turan[1]

The defects identified in the mechanical activity of the hearts from type 1 diabetic animals include alteration of Ca^{2+} signaling via changes in critical processes that regulate intracellular Ca^{2+} concentration. These defects result partially from a dysfunction of cardiac ryanodine receptor calcium release channel (RyR2). The present study was designed to determine whether the properties of the Ca^{2+} sparks might provide insight into the role of RyR2 in the altered Ca^{2+} signaling in cardiomyocytes from diabetic animals when they were analyzed together with Ca^{2+} transients. Basal Ca^{2+} level as well as Ca^{2+}-spark frequency of cardiomyoctes isolated from 5-week streptozotocin (STZ)-induced diabetic rats significantly increased with respect to aged-matched control rats. Ca^{2+} transients exhibited significantly reduced amplitude and prolonged time courses as well as depressed Ca^{2+} loading of sarcoplasmic reticulum in diabetic rats. Spatio-temporal properties of the Ca^{2+} sparks in cardiomyocytes isolated from diabetic rats were also significantly altered to being almost parallel to the changes of Ca^{2+} transients. In addition, RyR2 from diabetic rat hearts were hyperphosphorylated and protein levels of both RyR2 and FKBP12.6 depleted. These data show that STZ-induced diabetic rat hearts exhibit altered local Ca^{2+} signaling with increased basal Ca^{2+} level. ***Diabetes*** **54:3082–2088, 2005**

Diabetic cardiomyopathy as a distinct entity was first recognized by Rubler et al. (1) in diabetic patients with congestive heart failure who had no evidence of coronary atherosclerosis. Both electrical and mechanical properties of the myocardium from diabetes are significantly impaired (2–5). Ventricular myocardium from diabetic rats exhibits a reversible decrease in the speed of contraction, prolongation of contraction, and a delay in relaxation.

Contraction is initiated when a small amount of Ca^{2+} entering into the cell following membrane depolarization triggers a larger release of Ca^{2+} from the sarcoplasmic reticulum (SR). Spontaneous local Ca^{2+} transients, or Ca^{2+} sparks, are short-lived Ca^{2+} release events that are believed to demonstrate the main events of excitation-contraction in cardiomyocytes (6,7). The global increase in the amount of free Ca^{2+} in cardiomyocyte during depolarization consists of the summation of these unitary Ca^{2+} release events in cardiomyocytes (8) and skeletal muscle (9). On the other hand, it is generally agreed that any alteration of Ca^{2+} signaling could be a main source of cardiomyopathy (10). Since the Ca^{2+} flux underlying the Ca^{2+} sparks reports the summation of ryanodine-sensitive Ca^{2+} release channel (RyR2) behavior in the spark cluster, evaluation of the properties of the Ca^{2+} sparks may provide insight into the role of RyR2 in the altered Ca^{2+} signaling in cardiomyocytes from diabetic animals (3,4, 11,12).

Depression in contraction and relaxation of myocytes isolated from streptozotocin (STZ)-induced diabetic rats was found in parallel with reduced rate of rise and decline of intracellular Ca^{2+} transient elicited by electrical stimulation (5). These effects were mostly attributed to anomalous SR pump activity (11) and SR Ca^{2+} storage (3) and in part to reduced Na^{+}/Ca^{2+} exchange (13) and RyR2 protein expression. However, a change in RyR2 expression was not observed in this same model (14) nor in the diabetic *db/db* mouse (15). It rather was proposed that the RyR2 properties are altered. Dysfunction of RyR2 induced by diabetes could be, in part, due to formation of disulfide bonds between adjacent sulfhydryl groups (16), while chronic diabetes increases advanced glycation end products (16,17).

The goal of the present study was to specifically examine the behavior of the RyR2 receptors in diabetic rats. We reported here for the first time that local Ca^{2+} release events (Ca^{2+} sparks) in ventricular cardiomyocytes from STZ-induced diabetic rats are slower and have higher frequency with respect to the controls, consistent with alterations in Ca^{2+} handling and cardiac dysfunction. The changes in RyR2 opening kinetics could be related to hyperphosphorylation of RyR2 and FKBP12.6 release.

RESEARCH DESIGN AND METHODS

Diabetes was induced by a single intraperitoneal injection of STZ (50 mg/kg body wt and dissolved in 0.1 mol/l citrate buffer, pH 4.5) in adult male Wistar rats (200–250 g body wt). Control rats received citrate buffer alone. One week after injection of STZ, blood glucose levels were measured, and rats with blood glucose at least three times higher than the preinjection levels were used. All rats had free access to standard rat diet and water. All animals were used 5 weeks after STZ or citrate buffer injections. All experiments were performed in accordance with Ankara University School of Medicine ethics guidelines for the care and use of laboratory animals.

From the [1]Department of Biophysics, School of Medicine, Ankara University, Ankara, Turkey; the [2]Department of Pharmacology, School of Medicine, Ankara University, Ankara, Turkey; the [3]Department of Biophysics, School of Medicine, Hacettepe University, Ankara, Turkey; and [4]INSERM U-637, Physiopathologie Cardiovasculaire, CHU Arnaud de Villeneuve, Montpellier, France.

Address correspondence and reprint requests to Dr. Belma Turan, Department of Biophysics, School of Medicine, Ankara University, Ankara, Turkey. E-mail: belma.turan@medicine.ankara.edu.tr.

RyR2, ryanodine receptor Ca release channel; SR, sarcoplasmic reticulum; STZ, streptozotocin.

Received for publication 11 May 2005 and accepted in revised form 4 August 2005.

© 2005 by the American Diabetes Association.

The costs of publication of this article were defrayed in part by the payment of page charges. This article must therefore be hereby marked "advertisement" in accordance with 18 U.S.C. Section 1734 solely to indicate this fact.

Cell isolation. Hearts were removed rapidly and weighted after rats had been anesthetized with sodium pentobarbital (30 mg/kg body wt). Hearts were cannulated on a Langendorff apparatus and perfused retrogradely through the coronary arteries with a Ca^{2+}-free solution (in mmol/l): 145 NaCl, 5 KCl, 1.2 $MgSO_4$, 1.4 Na_2HPO_4, 0.4 NaH_2PO_4, 5 HEPES, and 10 glucose (pH 7.4), bubbled with O_2 at 37°C. Hearts were perfused for 3–5 min to clean out the remaining blood; this was followed by perfusion with the same solution containing 1 mg/ml collagenase (Collagenase A, Boehringer) for 30–35 min. Ventricles were then removed and minced into small pieces and gently massaged through a nylon mesh, and dissociated cardiomyocytes were washed with the collagenase-free solution. The percentage of viable cells was >70% in either group. Subsequently, Ca^{2+} was increased in a graded manner to a concentration of 1 mmol/l. Cells were kept in this solution at 37°C until used in the experiments. The percentage of Ca^{2+}-tolerant cells was ~60%.

Global cytosolic Ca^{2+} measurement. Intracellular Ca^{2+} transients were measured by fura-2 fluorescence at room temperature (21 ± 2°C). The cells were incubated at 37°C for 50 min with 4 μmol/l fura-2 AM for loading and then washed with fresh buffer. Fluorescence was recorded using a PTI Ratiomaster microspectrophotometer and FELIX software (Photon Technology International). Cells were excited at 340/380 nm and emission measured at 510 nm. The fluorescence ratio $F_{340/380}$ of the emitted light on excitation at 340 and 380 nm was calculated and used as an indicator of $[Ca^{2+}]_i$. $F_{340/380}$ ratio was measured at a frequency of 10 Hz. The composition of the bath solution used in $[Ca^{2+}]_i$ measurement was as follows (mmol/l): 130 NaCl, 4.8 KCl, 1.2 $MgSO_4$, 1.5 $CaCl_2$, 1.2 KH_2PO_4, 10 HEPES, and 10 glucose (pH 7.4). Following monitoring $[Ca^{2+}]_i$ for 20 s at rest, field-stimulation pulses of 20–30 V with 10-ms duration, were applied at 0.2-Hz frequency. Peak amplitude (difference between basal and peak $F_{340/380}$ ratios), time to peak, and half-decay time were determined from Ca^{2+} transients evoked by field stimulation. Background fluorescence measured from a cell-free field was subtracted from all recordings before calculation of ratios.

Caffeine-induced Ca^{2+} transients were induced by bath application of 10 mmol/l caffeine on cardiomyocytes 30 s after stopping field stimulation of the cells with electrical pulses (for 2 min at 0.2-Hz stimulation frequency) to ensure stable SR Ca^{2+} load.

L-Type Ca^{2+} current. Ca^{2+} currents (I_{CaL}) were recorded at room temperature (22 ± 2°C) using the whole-cell configuration of the patch clamp technique in the presence of cesium to inhibit K^+ currents and using voltage ramp by using a patch-clamp amplifier (Model RF-300; Biologic, Claix, France) and filtered at 3 kHz. Current traces were digitized at 5 kHz using Digidata 1200 and pClamp 8 software (Axon Instruments, Foster City, CA). The electrode resistance was 1.2–1.5 mol/lΩ.

Pipette solution for I_{CaL} contained (in mmol/l): 120 CsCl, 6.8 $MgC1_2$, 5.0 phosphocreatine-Na_2, 5.0 ATP-Na_2, 11 EGTA, and 20 HEPES (pH 7.2). The bathing solution for Ca^{2+} currents contained (in mmol/l): 117 NaCl, 1.7 $MgCl_2$, 5.4 $CsCl_2$, 10 HEPES, 1.8 $CaCl_2$, and 11 glucose (pH adjusted to 7.4 with NaOH). I_{CaL} was recorded during 250-ms depolarizing pulses to potentials between −50 and +60 mV (with 10-mV steps) applied at a frequency of 0.2 Hz after a 500-ms ramp to −45 mV from a holding potential of −80 mV. Current amplitude was estimated as the difference between peak inward current and the current level at the end of the 250-ms pulse.

Ca^{2+} spark measurement. Cardiomyocytes were placed into the recording chamber, which was set onto the stage of an inverted microscope equipped with a laser scanning confocal microscope (200 mol/l; LSM-Pascal, Zeiss, Germany). In the experiments, 40× (NA 1.3) oil immersion objectives were used for imaging cardiomyocytes located over the cover glass base of the recording chamber. A 488-nm laser line from an argon laser (25 mW) was used to excite the Ca^{2+}-sensitive dye, Fluo-3, and emitted fluorescence collected at 505 nm. Changes in $[Ca^{2+}]_i$ were recorded in line-scan mode (spatial [x] vs. temporal [t], 1.9 ms/line). To prevent photo-bleaching and cell damage, the laser line was kept at 4–6% of maximal intensity and the confocal pinhole set to 1–1.5 airy units to achieve the best resolution and emission intensity.

Image analysis was performed using LSM Image Examiner. The F value for fluorescence intensity of image was calculated by averaging pixels other than potential spark areas. Then $\Delta F/F$ image was created by using this F value. Ca^{2+} sparks were manually detected and converted to temporal lines by averaging fluorescence intensity of 2–3 pixels aligning the peak of fluorescence intensity over time. The signals were filtered using a Butterworth digital filter. The temporal profiles were then fitted to gamma function to analyze time to peak, peak amplitude of fluorescence intensity, and decrease time to half-maximum.

Western blot analysis. Hearts were homogenized with a motor-driven Teflon-to-glass homogenizer in cold Tris-HCl buffer containing (in mmol/l): 50 Tris-HCl (pH 7.4), 200 NaCl, 20 NaF, 1.0 Na_3VO_4, 1 dithiothreitol, and protease inhibitors (complete tablet from Roche) and centrifuged at 1000g for 30 min at 4°C. Supernatant was centrifuged at 30,000g for 30 min, then at 100,000g for 1 h at 4°C. Pellet was suspended with the homogenization buffer and protein amount measured (18). The samples (100 μg protein) were subjected to 5% SDS-PAGE for RyR2 assay and 10% SDS-PAGE for both FKBP12.6 and actin assays and then transferred electrophoretically to nitrocellulose membrane. Immunoblotting was performed using antibodies against RyR2, RyR2-P (kind gift of Drs. A. Marks and X. Wehrens; dilutions 1/5,000 and 1/3,000, respectively), FKBP12.6, and actin (Santa Cruz), and then enhanced chemoluminescence. Briefly, nitrocellulose membranes were incubated 1 h at 4°C in PBS (20 mmol/l NaH_2PO_4-Na_2HPO_4, pH 7.6, containing 154 mmol/l NaCl, 3% BSA, and 8% nonfatty dry milk). Blots were washed several times with PBS containing 0.1% Tween and then incubated with antiserum at room temperature for 1–2 h by shaking. Blots were then washed several times with PBS, incubated with horseradish peroxidase–labeled anti-rabbit IgG (Santa Cruz Biotech, Santa Cruz, CA) (dilution 1/10,000) for 1 h at room temperature. Blots were washed several times with PBS and then incubated with ECL Western blotting reagent (Amersham, Vienna, Austria) for 1 min and exposed to X-ray film for 45–90 s.

RESULTS

General characteristics of STZ-induced diabetic rats. Diabetic animals had significantly high glucose levels (458 ± 8 mg/dl) compared with control animals (101 ± 1 mg/dl). They stopped gaining weight (213.6 ± 9.2 vs. 197.8 ± 7.9 g) following STZ injection, while control animals continued to gain weight (215.0 ± 4.9 vs. 249.2 ± 6.8 g) at the end of the 5-week experimental period. The heart weight–to–body weight ratio was 4.08 ± 0.58 vs. 4.04 ± 0.38 mg/g in the diabetic versus control groups. To avoid the possible insensitive heart-weight measurement, we also measured the capacitance of the isolated cardiomyocytes and compared the values between the groups. The mean cell capacitances of the control and diabetic rats were similar as previously reported (189.9 ± 12.2 and 180.6 ± 13.6 pF, respectively) (19).

Global Ca^{2+} homeostasis in diabetic rat heart. Figure 1*A* shows original recordings of Ca^{2+} transients elicited in control and diabetic rat cardiomyocytes. The averaged peak amplitude of $\Delta F_{340/380}$ was significantly smaller in diabetic than in control cells (0.23 ± 0.01 and 0.35 ± 0.02 AU, respectively) (Fig. 1*B*). The time to peak amplitude of Ca^{2+} transients of diabetic cells (0.26 ± 0.01 s) was significantly larger than the control ones (0.18 ± 0.01 s), and the half-time for recovery, half-decay time was significantly prolonged with respect to the controls (0.64 ± 0.02 vs. 0.50 ± 0.02 s).

The averaged diastolic values of $\Delta F_{340/380}$ were 0.49 ± 0.01 and 0.41 ± 0.01AU in diabetic and control groups, respectively ($P < 0.001$). This is indicative that the basal $[Ca^{2+}]_i$ level is larger in the diabetic groups (Fig. 1*C*).

L-Type Ca^{2+} currents. To determine whether a change in L-type Ca^{2+} currents (I_{CaL}) contributes to the altered Ca^{2+} sparks activity observed in the diabetic group with respect to the control group in the present study, I_{CaL} was examined with whole-cell patch-clamp technique. The densities of I_{CaL} of both groups were similar at all voltages from −50 to +60 mV. The average peak current densities measured at 0 mV are given in Fig. 1*D*. Besides the amplitudes (10.9 ± 0.7 and 10.2 ± 0.5 pA/pF in control vs. diabetes, respectively), the fast and slow activation time constants of I_{CaL} (8.1 ± 1.2, 52.9 ± 7.1, and 7.6 ± 1.9 ms; 54.9 ± 5.8 ms in control vs. diabetes) obtained by fitting a two-exponential curve (17) were found to be similar (Fig. 1*D*, *inset*). The current voltage relationships of I_{CaL} of both groups recorded between −50 and +60 mV were similar as well (data not shown). This result demonstrates that L-type Ca^{2+} channel function was not significantly different due to diabetes.

Local SR Ca^{2+} release in diabetic rat heart. Ca^{2+} sparks, which represent SR Ca^{2+} release from clusters of

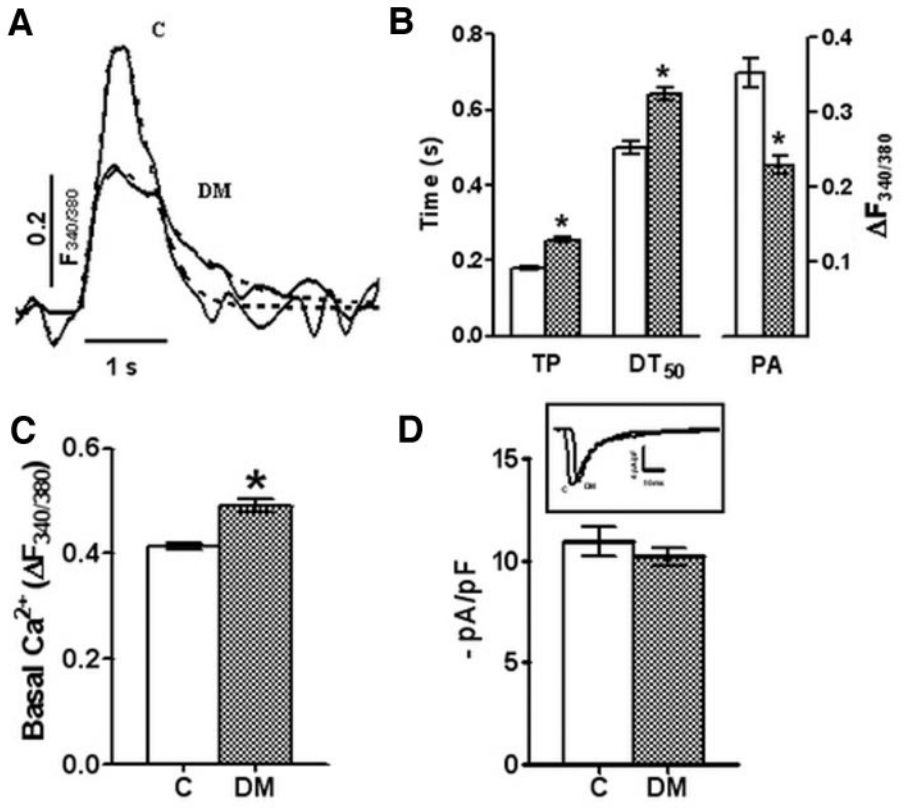

FIG. 1. Ca^{2+} transients and basal intracellular $[Ca^{2+}]_i$ are changed in cardiomyocytes from diabetic rats. *A*: Representative Ca^{2+} transients and fitted curves (dashed lines) of diabetic (DM) and control (C) rat cardiomyocytes field stimulated at 0.2 Hz. *B*: Bar graphs representing the changes in peak amplitude (PA) of the fluorescence $[Ca^{2+}]_i$ transients ($\Delta F_{340/380} = F_{340/380}$ peak $- F_{340/380}$ basal), time to peak (TP), and decay time to 50% of the peak transient (DT_{50}) of the diabetic ($n_{rat} = 5$, $n_{cell} = 25$) and control groups ($n_{rat} = 5$, $n_{cell} = 24$). *C*: Change of basal $[Ca^{2+}]_i$ in the diabetic group with respect to the control group. *D*: Comparison of L-type Ca^{2+} currents (I_{CaL}) recorded in cardiomyocytes from diabetic (dashed line) and control rat (continuous line) hearts. *Inset*: representative current records, time shifted for clarity. Currents were recorded by applying 250-ms depolarizing voltage steps at 0.2 Hz from a holding potential of −80 to 0 mV. The current amplitude was estimated as the difference between peak inward current and the current level at the end of the 250-ms pulse and normalized to cell capacitance. Values are expressed as means ± SE of 10–12 cells from at least five rats. *$P < 0.001$ vs. control.

RyR2, were examined in cardiomyocytes isolated from control and STZ-induced diabetic rat hearts. Representative line-scan images of the cardiomyocytes from the control and the diabetic rats (individual Ca^{2+} spark image x vs. t) are displayed in Fig. 2*A*. Representative temporal and averaged spatial profiles of Ca^{2+} sparks recorded in cells from a control and a diabetic rat are given in Fig. 2*B*. The spatial time courses were extracted as the mean of all recorded spatial or temporal pixels centered at the peak of the $\Delta F/F$ of the Ca^{2+} spark. These transients were then fitted by a gamma distribution function to obtain objective kinetic and spatial measures of the events (19).

Quantitative data for Ca^{2+} spark characteristics are summarized in Fig. 2*C*. Peak amplitude determined as

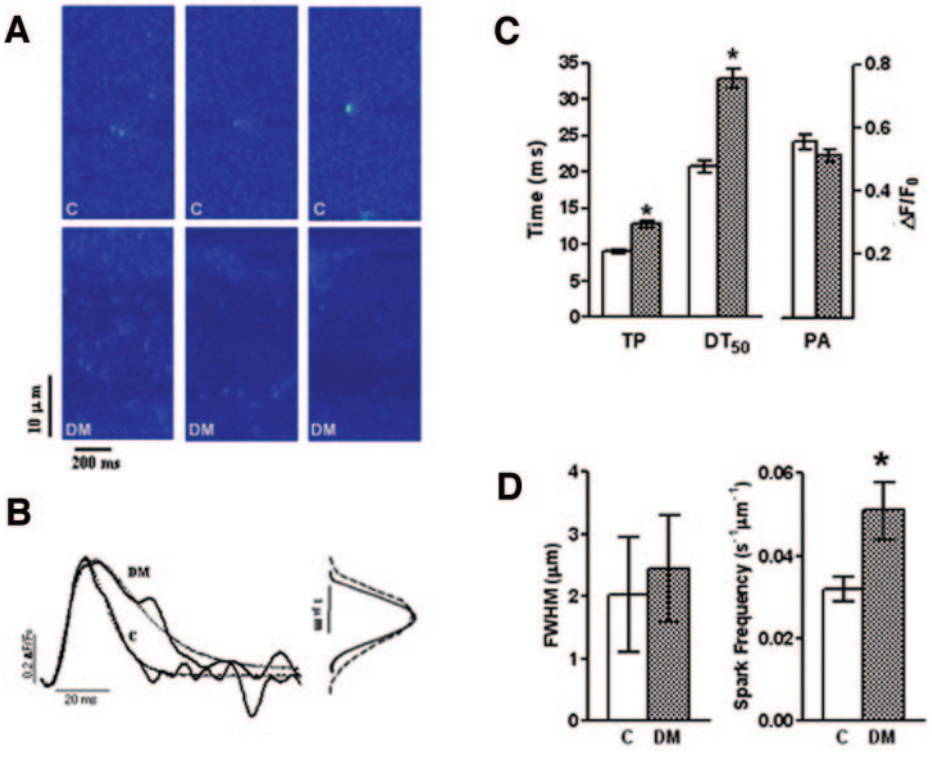

FIG. 2. Spatio-temporal properties of Ca^{2+} sparks in diabetes. *A*: Representative line-scan images of isolated cardiomyocytes. C, control; DM, diabetic. *B*: Averaged spatial profiles of Ca^{2+} sparks (*continues line*: C, *dashed line*: diabetic) (*right panel*) and temporal profiles together with fitted curves (dashed line) of a spark from both groups (*left panel*). *C*: Time to peak amplitude (TP), half decay-time (DT_{50}), and peak amplitude (PA) of Ca^{2+} sparks measured in control (C) and diabetic (DM) rat cardiomyocytes ($n_{rat} = 5$, $n_{cell} = 34$, $n_{spark} = 152$ vs. $n_{rat} = 4$, $n_{cell} = 25$, $n_{spark} = 145$ in diabetic vs. control). *D*: Spatial distribution of the sparks (frequency of Ca^{2+} sparks width at half their maximal amplitude [FWHM]) (*left panel*) and comparison of Ca^{2+} sparks frequency (10 vs. 12 cardiomyocytes from control [C] vs. diabetic [DM] groups) (*right panel*). *$P < 0.0001$ vs. control.

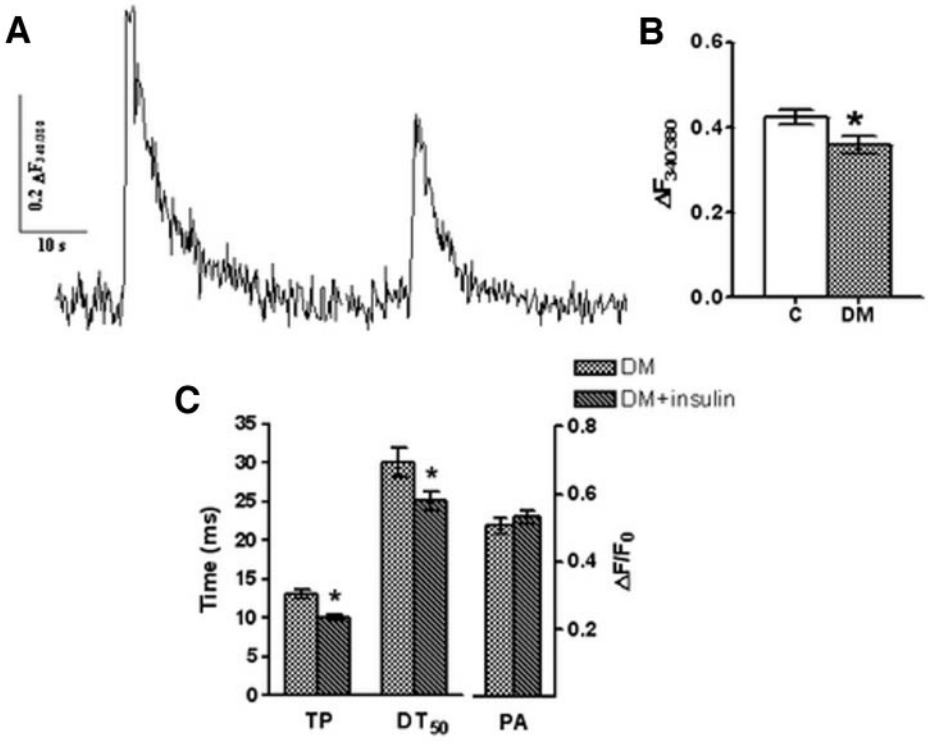

FIG. 3. Effect of diabetes on caffeine response. *A*: Representative tracings of caffeine-induced peak intracellular Ca^{2+} transients elicited in cardiomyocytes isolated from control (*C*) and diabetic (DM) animals. Traces have been shifted for sake of clarity. *B*: $\Delta F_{340/380}$ values of the two groups. Values are expressed as means ± SE of 12–17 cells from at least five animals. *$P < 0.01$ vs. control. *C*: Recovery of altered parameters of Ca^{2+} sparks following 100-nmol/l insulin incubation for 4–5 h at 37°C. Values are expressed as means ± SE of 58 cells (insulin incubated, two diabetic rats) vs. 45 cardiomyocytes (nonincubated, two diabetic rats). *$P < 0.001$ vs. nonincubated.

$\Delta F/F$ at the peak of Ca^{2+} spark, frequency of Ca^{2+} sparks width at half-maximal amplitude, time to peak, and time to half decrease were calculated from individual gamma distribution function fits. The mean peak amplitude of the diabetic group ($\Delta F/F$) was not changed (0.51 ± 0.02 and 0.56 ± 0.02 AU in diabetic and control, respectively), but time to peak was significantly slower (12.88 ± 0.50 and 9.08 ± 0.30 ms in diabetic and control groups, respectively) as well as time to half decrease, which prolonged from 20.78 ± 0.87 to 32.90 ± 1.29 ms with respect to the control group ($P < 0.0001$). The spatial spread (frequency of Ca^{2+} sparks width at half-maximal amplitude) was not significantly different in the diabetic group with respect to the control group (2.45 ± 0.85 vs. 2.05 ± 0.92 μm) (Fig. 2*D*, *left*). Spontaneous Ca^{2+} sparks frequency was higher ($P < 0.0001$) in diabetic cardiomyocytes (0.051 ± 0.007 $s^{-1}\mu/m^{-1}$) than in the control cells (0.032 ± 0.003 $s^{-1}\mu/m^{-1}$) (Fig. 2*D*, *right*).

SR Ca^{2+} content of cardiomyocytes. Caffeine application caused a sudden and transient increase in intracellular Ca^{2+} of cardiomyocytes due to Ca^{2+} release from SR. The size of the caffeine-induced Ca^{2+} transient has been used to assess the SR Ca^{2+} load of control and diabetic cardiomyocytes. To assure stable SR Ca load, cells were first stimulated and caffeine (10 mmol/l) rapidly applied 30 s after cessation of electrical stimulation. The caffeine-induced Ca^{2+} transient recorded in cardiomyocytes from diabetic rats was smaller than the corresponding control one (Fig. 3*A*). The averaged caffeine responses ($\Delta F/F$) were 0.42 ± 0.02 vs. 0.36 ± 0.02 AU in the control versus diabetic cells, and the difference between these two groups is statistically significant (Fig. 3*B*).

Effects of insulin on Ca^{2+} sparks. To clarify whether the altered parameters of Ca^{2+} sparks arise due to STZ-induced diabetes (type 1, insulin-dependent diabetes) or a result of the direct toxic effect of STZ on cardiomyocytes, cells from diabetic rats were incubated in the presence or not of insulin (100 nmol/l) for 4–5 h at 37°C. Then, we recorded Ca^{2+} sparks and calculated the time to peak and the time to half decrease of the sparks. The mean peak amplitudes of the sparks ($\Delta F/F$) from these two groups of cells were not affected by insulin incubation, but the time to peak of the insulin incubated group of cells (58 sparks in five cells from two rats) was significantly recovered (10.06 ± 0.30 vs. 13.03 ± 0.52 ms) compared with untreated cells (45 sparks in four cells from two rats). Also, time to half increase was recovered from 30.04 ± 1.81 to 25.06 ± 1.19 ms ($P < 0.001$). If we compare these parameters with those from normal controls (time to peak 9.08 ± 0.30 ms, time to half decrease 20.78 ± 0.87 ms), we can see significant recoveries with insulin incubation of the cardiomyocytes from STZ-induced diabetic rats (Fig. 3*C*).

Biochemical analysis of RyR2 in diabetes. The mechanisms underlying the dysfunction of RyR2 in diabetes remain undefined. We hypothesized that the alterations in Ca^{2+} release behavior seen at the global and local spark level in STZ-induced diabetic rat cardiomyocytes could be due to a defect in RyR2 function following its phosphorylation and release of FKBP12.6, an accessory protein of RyR2 macromolecular complex, as documented in heart failure (20). The phosphorylation level of RyR2 in diabetic and control rat heart tissue was evaluated using specific antibodies directed against RyR2 and phosphorylated RyR2 (Fig. 4*A*). Total RyR2 in the diabetic groups was ~44% less than in the control group as estimated from the Western-blot bands (Fig. 4*B*). There is strong evidence of phosphorylation of RyR2 in diabetic rat heart but no appearance of it in the control rat hearts. The amount of FKBP12.6 was decreased by 41% in the diabetic rat heart compared with the control rat heart (Fig. 4*B*). There was no significant difference in the protein levels of actin in diabetic and control groups (Fig. 4*B*).

DISCUSSION

This study on STZ-induced type 1 diabetes in rats reports significant alterations in Ca^{2+} homeostasis that can ac-

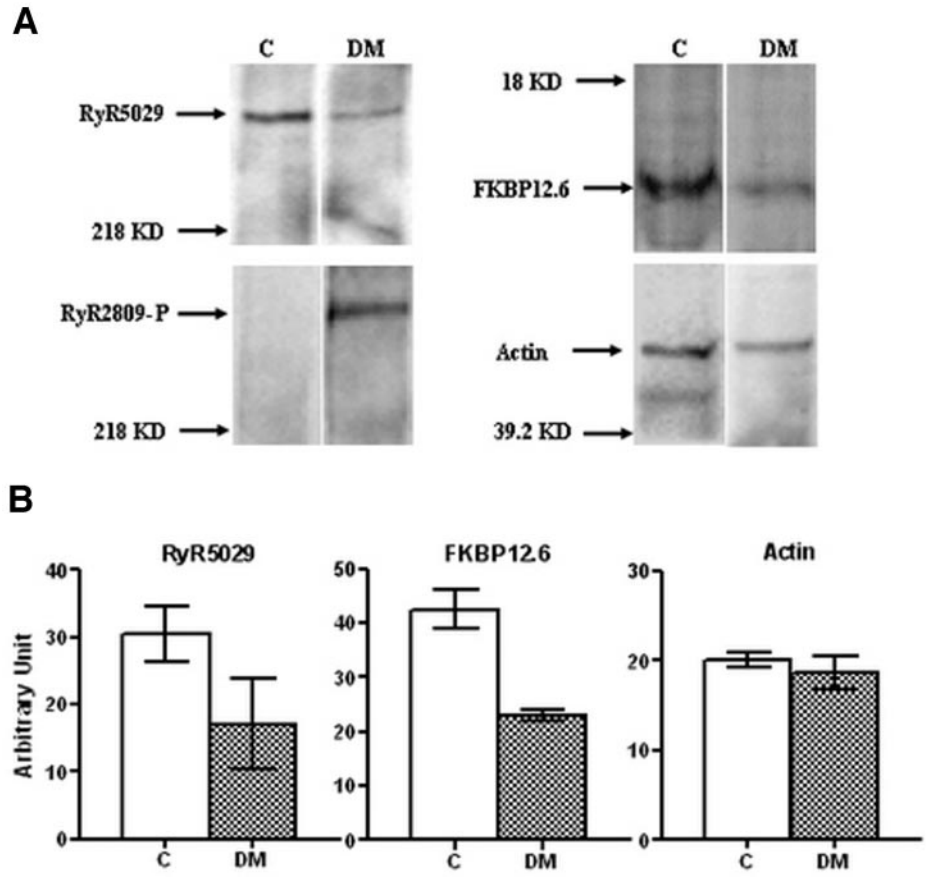

FIG. 4. Amount and phosphorylated level of RyR2. *A*: Representative Western blots of RyR2, RyR2-P, FKBP12.6, and actin in control (C) and diabetic (DM) rats. *B*: The average changes of both RyR2 and FKBP12.6 are 44 and 41%, respectively, vs. control, while there was no significant change in actin level (at least two animals with double assays in each sample from each group for each type of measurement). *$P < 0.05$ vs. control.

count for the well-known contractile dysfunction in such pathological conditions. At first we confirmed the defective intracellular Ca^{2+} signaling with both lower amplitude and slower kinetics of Ca^{2+} transients as well as the decreased SR Ca^{2+} load (5). Furthermore, we clearly established that these defects could be attributed to anomalous RyR2 behavior, as revealed by the spatio-temporal properties of Ca^{2+} sparks that especially exhibited slower kinetics. The reduced amount of RyR2 and FKBP12.6 levels and the protein kinase A–dependent phosphorylation of RyR2 could be responsible for most of these observations. A lower SR Ca^{2+} load reinforced these defects in Ca^{2+} release channel properties.

The diabetic cardiomyopathy, starting with asymptomatic left ventricular diastolic dysfunction, progresses to compromised systolic function that leads to increased incidence in morbidity and mortality. Coincident with the alteration of cardiac function are a variety of metabolic and biochemical abnormalities that include change in the predominance of myosin isoenzymes (21), an activity of the SR Ca^{2+}-ATPase (3,5,11,22,23). In addition, diabetes has been associated with a reversible increase in the duration of the action potential attributable to a reduced transient outward K^+ current (I_{K1}), while the L-type Ca^{2+} current (I_{CaL}) was unaffected (5,24–26). Thus, diabetes exhibits some similarities with heart failure in which it has been reported that I_{K1} is reduced as a consequence of elevated diastolic Ca^{2+} following altered RyR2 properties (27).

Despite the fact that I_{CaL} is not modified by diabetes, the cardiomycytes from diabetic rats demonstrate significant alterations in Ca^{2+} homeostasis. These include increases in rise time and half-decay time of Ca^{2+} transient together with decrease in Ca^{2+} transient amplitude and SR Ca^{2+} load as well as increase in diastolic Ca^{2+}. All these changes could be consequent to the alterations in RyR2 behavior that we describe here. The decrease in SR Ca^{2+} load has been reported in several previous studies (5) and was already suggested by rapid cooling contracture experiments (28). This is attributable to reduced sarcoplasmic reticulum Ca-ATPase and increased phospholamban expression (29,30) as well as to the anomalous RyR2 activity. These factors could also be responsible for the larger diastolic Ca^{2+} level seen here in diabetic cells (31–33), although others reported no change (34,35) or even a decrease (36,37). However, this latter work (37) was performed using a low-Ca (0.5 mmol/l)–containing extracellular solution. It needs to be emphasized that the current controversy in resting Ca^{2+} levels in both tissue and isolated myocytes in diabetic hearts is under consideration and needs to be clarified with additional data.

Our data also show that insulin incubation of the cardiomyocytes from diabetic rats for 4 h significantly restored the altered parameters of Ca^{2+} sparks and thus provides support for the origin of these alterations. It is well known that STZ can induce cardiac dysfunction depending on insulin deficiency (type 1 diabetes), while insulin treatment of these animals/cells could recover almost all of these parameters (25,28,38–41). Besides these published data, it has been shown that altered SR Ca^{2+}content and RYR2 binding, altered SR protein expression, as well as altered RyR2 mRNA levels and RyR2 protein levels (5,14,17) were normalized following insulin treatment of the STZ-induced diabetic animals in vivo and/or in vitro.

It is now well documented that an increase in $[Ca^{2+}]_i$ is

one of the major steps in the sequences of events leading to contraction of cardiac muscle. These sequences of events are demonstrated in part by Lopez-Lopez et al. (7), in which we have shown that parallel defects in contraction and $[Ca^{2+}]_i$ transients in our diabetes model clearly indicate that defective intracellular Ca^{2+} signaling contributes to contractile dysfunction in diabetes. In our diabetes model, although there is significant prolongation in action potential duration as well as delayed rise time and prolonged decay in contractile activity, the density of I_{CaL} was similar at all voltages from −50 to +60 mV, and L-type Ca^{2+} channel function did not show any difference due to diabetes (5,26). Therefore, it is concluded that I_{CaL} did not contribute to the altered activity of $[Ca^{2+}]_i$ transient observed in the diabetic group; rather, the gain of function of the excitation-contraction coupling is markedly decreased.

In addition to the changes in $[Ca^{2+}]_i$ transients, here we report alterations in the properties of spontaneous Ca^{2+} sparks in cardiomyocytes from diabetic rats. Populations of Ca^{2+} sparks from diabetic rat cardiomyocytes have significantly slower temporal kinetics. It has been demonstrated in skeletal muscle that the rising phase of the Ca^{2+} spark fluorescence represents the underlying open time of RyR Ca^{2+} channels (9). This similar conclusion could be made in cardiomyocytes. Alternatively, the decay phase of spark fluorescence is characterized by the diffusion of Ca^{2+} away from the SR and is thought to be independent of SERCA activity. Thus, the spark decay may be influenced by intrinsic Ca^{2+} buffering processes (42).

The Western blot analysis supports altered activity of RyR2 in diabetes. There are, however, controversies about the RyR2 properties in diabetes. Similar data were published by Guatimosim et al. (12) and Bidasee et al. (14). They have mentioned the importance of evaluation of the properties of the Ca^{2+} sparks as insight into the role of RyR2 in the altered Ca^{2+} signaling in diabetic cardiomyocytes. Their data have also shown that although expression did not change significantly after 6 weeks of diabetes, the ability of RyR2 to bind the specific ligand [^{3}H]ryanodine was significantly lowered (14). These authors also demonstrated that chronic diabetes (8 weeks) induced a decrease in cardiac contractility in part due to a decrease in expression and an alteration in function of RyR2 (16).

Another origin of altered parameters of Ca^{2+} signaling might be the deficiency in SR Ca^{2+} load. Indeed, a similar application of caffeine released a significantly less amount of Ca^{2+} from SR, in agreement with previous results by Choi et al. (5) in a similar diabetes model. These studies, therefore, identify important alterations in SR function due to either a decreased level and altered function of RyR2 and/or a depressed level of SERCA.

RyR2 receptors are regulated by a variety of proteins, including FKBP12.6. Due to its importance in the coupled gating of RyR2, its deficit and alteration has been involved in heart failure. However, there are controversies related to its effects on Ca^{2+} spark parameters (20,43,44). Our data showed that kinetic parameters of Ca^{2+} sparks are slower in diabetic compared with control rats. These alterations are due to defects in RyR2 receptor behavior. According to the RyR2-coupled gating hypothesis (45), FKBP12.6 allows all RyR2 clusters to open and close simultaneously. Therefore, any type of alteration in this protein, associated here with a decreased amount of RyR2, will cause a depression in both time to peak and time to half decrease of Ca^{2+} sparks. The question thus arises as to how less RyR2 and FKBP12.6 and phosphorylated RyR2 can cause no significant change in the amplitude of Ca^{2+} transient together with significant prolongations in both time to peak and time to half decrease. This effect is may be due to leaky SR in diabetes. This hypothesis is consistent with several studies and also supported by our data on both increased basal Ca^{2+} level and Ca^{2+} spark frequency in diabetes (5,15,46). A further study on quantitative assessment of RyR2 and FKBP12.6 mRNA levels of hearts from control and diabetic groups is needed to fully clarify their roles in excitation-contraction coupling and its alteration during diabetes.

These alterations in Ca^{2+} homeostasis might be responsible for heart remodeling that occurs without significant cell growth. Like most others (25,47), we observed no change in membrane capacitance, while after longer STZ-treatment of younger rats, Choi et al. (5) observed a decrease in membrane capacitance. This was associated with a lack of increase in body weight during the 5 weeks of STZ treatment that indicates a relative cell hypertrophy in diabetic rats. This is in line with the increase in heart weight–to–body weight ratio previously reported (23,48).

In summary, we have demonstrated that cardiac contractile dysfunction is closely related to altered Ca^{2+} signaling as well as altered electrical activity. Therefore, it has been demonstrated for the first time that altered parameters of both Ca^{2+} transients and Ca^{2+} sparks are responsible for the altered Ca^{2+} signaling in diabetes, and these alterations may be in part associated with not only less Ca^{2+} loading of SR, but also phosphorylation of RyR2 in diabetes.

ACKNOWLEDGMENTS

This work has been supported by grants from Ankara University Biotechnology Institute (project no. 2001K120-240) and the Turkish Scientific and Technical Research Council (project no. 104S591).

We thank Drs. A.M. Marks and X. Wehrens for the generous gift of RyR2 and RyR2-P antibodies.

REFERENCES

1. Rubler S, Dlugash J, Yuceoglu YZ, Kumral T, Branwood AW, Grishman A: New type of cardiomyopathy associated with diabetic glomerulosclerosis. *Am J Cardiol* 30:595–602, 1972
2. Fein FS, Sonnenblick EH: Diabetic cardiomyopathy. *Cardiovasc Drugs Ther* 8:65–73, 1994
3. Bouchard RA, Bose D: Influence of experimental diabetes on sarcoplasmic reticulum function in rat ventricular muscle. *Am J Physiol* 260:H341–H354, 1991
4. Pierce GN, Kutryk MJ, Dhalla NS: Alterations in Ca2+ binding by and composition of the cardiac sarcolemmal membrane in chronic diabetes. *Proc Natl Acad Sci U S A* 80:5412–5416, 1983
5. Choi KM, Zhong Y, Hoit BD, Grupp IL, Hahn H, Dilly KW, Guatimosim S, Lederer WJ, Matlib MA: Defective intracellular Ca(2+) signaling contributes to cardiomyopathy in type 1 diabetic rats. *Am J Physiol Heart Circ Physiol* 283:H1398–H1408, 2002
6. Cheng H, Lederer WJ, Cannell MB: Calcium sparks: elementary events underlying excitation-contraction coupling in heart muscle *Science* 262: 740–744, 1993
7. Lopez-Lopez JR, Shacklock PS, Balke CW, Wier WG: Local, stochastic release of Ca2+ in voltage-clamped rat heart cells: visualization with confocal microscopy. *J Physiol* 480:21–29, 1994
8. Lopez-Lopez JR, Shacklock PS, Balke CW, Wier WG: Local calcium transients triggered by single L-type calcium channel currents in cardiac cells. *Science* 268:1042–1045, 1995
9. Klein MG, Lacampagne A, Schneider MF: Voltage dependence of the pattern and frequency of discrete Ca2+ release events after brief reprimming in frog skeletal muscle *Proc Natl Acad Sci U S A* 94:11061–11066, 1997
10. Wehrens XH, Marks AR: Altered function and regulation of cardiac

ryanodine receptors in cardiac disease. *Trends Biochem Sci* 28:671–678, 2003
11. Ganguly PK, Pierce GN, Dhalla KS, Dhalla NS: Defective sarcoplasmic reticular calcium transport in diabetic cardiomyopathy. *Am J Physiol* 244:E528–E535, 1983
12. Guatimosim S, Dilly K, Santana LF, Saleet JM, Sobie EA, Lederer WJ: Local Ca(2+) signaling and EC coupling in heart: Ca(2+) sparks and the regulation of the [Ca(2+)](i) transient. *J Mol Cell Cardiol* 34:941–950, 2002
13. Schaffer SW, Ballard-Croft C, Boerth S, Allo SN: Mechanisms underlying depressed Na+/Ca2+ exchanger activity in the diabetic heart. *Cardiovasc Res* 34:129–136, 1997
14. Bidasee KR, Dincer UD, Besch HR Jr: Ryanodine receptor dysfunction in hearts of streptozotocin-induced diabetic rats. *Mol Pharmacol* 60:1356–1364, 2001
15. Belke DD, Dillmann WH: Altered cardiac calcium handling in diabetes. *Curr Hypertens Rep* 6:424–429, 2004
16. Bidasee KR, Nallani K, Besch HR Jr, Dincer UD: Streptozotocin-induced diabetes increases disulfide bond formation on cardiac ryanodine receptor (RyR2). *J Pharmacol Exp Ther* 305:989–998, 2003
17. Bidasee KR, Nallani K, Yu Y, Cocklin RR, Zhang Y, Wang M, Dincer UD, Besch HR Jr: Chronic diabetes increases advanced glycation end products on cardiac ryanodine receptors/calcium-release channels. *Diabetes* 52: 1825–1836, 2003
18. Bradford MM: A rapid and sensitive method for the quantitation of microgram quantities of protein utilizing the principle of protein-dye binding. *Anal Biochem* 72:248–254, 1976
19. Ozdemir S, Ugur M, Gurdal H, Turan B: Treatment with AT(1) receptor blocker restores diabetes-induced alterations in intracellular Ca(2+) transients and contractile function of rat myocardium. *Arch Biochem Biophys* 435:166–174, 2005
20. Marx SO, Reiken S, Hisamatsu Y, Jayaraman T, Burkhoff D, Rosemblit N, Marks AR: PKA phosphorylation dissociates FKBP12.6 from the calcium release channel (ryanodine receptor): defective regulation in failing hearts. *Cell* 101:365–376, 2000
21. Malhotra A, Penpargkul S, Fein FS, Sonnenblick EH, Scheuer J: The effect of streptozotocin-induced diabetes in rats on cardiac contractile proteins *Circ Res* 49:1243–1250, 1981
22. Fein FS, Kornstein LB, Strobeck JE, Capasso JM, Sonnenblick EH: Altered myocardial mechanics in diabetic rats. *Circ Res* 47:922–933, 1980
23. Zhong Y, Ahmed S, Grupp IL, Matlib MA: Altered SR protein expression associated with contractile dysfunction in diabetic rat hearts. *Am J Physiol Heart Circ Physiol* 281:H1137–H1147, 2001
24. Jourdon P, Feuvray D: Calcium and potassium currents in ventricular myocytes isolated from diabetic rats. *J Physiol* 470:411–429, 1993
25. Shimoni Y, Firek L, Severson D, Giles W: Short-term diabetes alters K+ currents in rat ventricular myocytes *Circ Res* 74:620–628, 1994
26. Yaras N, Turan B: Interpretation of relevance of sodium-calcium exchange in action potential of diabetic rat heart by mathematical model. *Mol Cell Biochem* 269:121–129, 2005
27. Fauconnier J, Lacampagne A, Rauzier JM, Vassort G, Richard S: Ca^{2+}-dependent reduction of I_{K1} in rat ventricular cells: a novel paradigm for arrhythmia in heart failure? *Cardiovasc Res.* In press
28. Yu Z, Tibbits GF, McNeill JH: Cellular functions of diabetic cardiomyocytes: contractility, rapid-cooling contracture, and ryanodine binding. *Am J Physiol* 266:H2082–H2089, 1994
29. Teshima Y, Takahashi N, Saikawa T, Hara M, Yasunaga S, Hidaka S, Sakata T: Diminished expression of sarcoplasmic reticulum Ca(2+)-ATPase and ryanodine sensitive Ca(2+)channel mRNA in streptozotocin-induced diabetic rat heart. *J Mol Cell Cardiol* 32:655–664, 2000
30. Choi KM, Barash I, Rhoads RE: Insulin and prolactin synergistically stimulate beta-casein messenger ribonucleic acid translation by cytoplasmic polyadenylation. *Mol Endocrinol* 18:1670–1686, 2004
31. Regan TJ, Wu C, Yeh C, Oldewurtel H, Haider B: Myocardial compositionand function in diabetes: the effects of chronic insulin use. *Circ Res* 49:1268–1277, 1981
32. Schaffer SW, Mozaffari MS, Artman M, Wilson GL: Basis for myocardial mechanical defects associated with non-insulin-dependent diabetes. *Am J Physiol* 256:E25–E30, 1989
33. Allo SN, Lincoln TM, Wilson GL, Green FJ, Watanabe AM, Schaffer SW: Non-insulin-dependent diabetes-induced defects in cardiac cellular calcium regulation. *Am J Physiol* 260:C1165–C1171, 1991
34. Eckel J, Gerlach-Eskuchen E, Reinauer H: Alpha-adrenoceptor-mediated increase in cytosolic free calcium in isolated cardiac myocytes. *J Mol Cell Cardiol* 23:617–625, 1991
35. Yu Z, Quamme GA, McNeill JH: Depressed [Ca2+]i responses to isoproterenol and cAMP in isolated cardiomyocytes from experimental diabetic rats. *Am J Physiol* 266:H2334–H2342, 1994
36. Bergh CH, Hjalmarson A, Sjogren KG, Jacobsson B: The effect of diabetes on phosphatidylinositol turnover and calcium influx in myocardium. *Horm Metab Res* 20:381–386, 1988
37. Noda N, Hayashi H, Miyata H, Suzuki S, Kobayashi A, Yamazaki N: Cytosolic Ca2+ concentration and pH of diabetic rat myocytes during metabolic inhibition. *J Mol Cell Cardiol* 24:435–446, 1992
38. Penpargkul S, Schaible T, Yipintsoi T, Scheuer J: The effects of diabetes on performance and metabolism of rat hearts. *Circ Res* 47:911–921, 1980
39. Magyar J, Rusznak Z, Szentesi P, Szucs G, Kovacs L: Action potentials and potassium currents in rat ventricular muscle during experimental diabetes. *J Mol Cell Cardiol* 24:841–853, 1992
40. Fein FS, Miller-Green B, Zola B, Sonnenblick EH: Reversibility of diabetic cardiomyopathy with insulin in rabbits. *Am J Physiol* 250:H108–H113, 1986
41. Shimoni Y, Rattner J: Type 1 diabetes leads to cytoskeletonchanges that are reflected in insulin action on rat cardiac K(+) currents. *Am J Physiol Endocrinol Metab* 281:E575–E585, 2001
42. Jiang YH, Klein MG, Schneider MF: Numerical simulation of Ca(2+) "Sparks" in skeletal muscle. *Biophys J* 77:2333–2357, 1999
43. Gomez AM, Schuster I, Fauconnier J, Prestle J, Hasenfuss G, Richard S: FKBP12.6 overexpression decreases Ca2+ spark amplitude but enhances [Ca2+]i transient in rat cardiac myocytes. *Am J Physiol Heart Circ Physiol* 287:H1987–H1993, 2004
44. Xin HB, Senbonmatsu T, Cheng DS, Wang YX, Copello JA, Ji GJ, Collier ML, Deng KY, Jeyakumar LH, Magnuson MA, Inagami T, Kotlikoff MI, Fleischer S: Oestrogen protects FKBP12.6 null mice from cardiac hypertrophy. *Nature* 416:334–338, 2002
45. Marx SO, Gaburjakova J, Gaburjakova M, Henrikson C, Ondrias K, Marks AR: Coupled gating between cardiac calcium release channels (ryanodine receptors). *Circ Res* 88:1151–1158, 2001
46. Zhu X, Bernecker OY, Manohar NS, Hajjar RJ, Hellman J, Ichinose F, Valdivia HH, Schmidt U: Increased leakage of sarcoplasmic reticulum Ca2+ contributes to abnormal myocyte Ca2+ handling and shortening in sepsis. *Crit Care Med* 33:598–604, 2005
47. Shimoni Y, Liu XF: Gender differences in ANG II levels and action on multiple K+ current modulation pathways in diabetic rats. *Am J Physiol Heart Circ Physiol* 287:H311–H319, 2004
48. Dincer UD, Bidasee KR, Guner S, Tay A, Ozcelikay AT, Altan VM: The effect of diabetes on expression of β1-, β2-, and β3-adrenoreceptors in rat hearts. *Diabetes* 50:455–461, 2001